ELSEVIER

Available online at www.sciencedirect.com

SciVerse ScienceDirect

Physics Procedia 27 (2012) 356 – 359

Physics Procedia

ISS2011

Operation of superconducting nano-stripline detector (SSLD) mounted on cryogen-free cryostat

Nobuyuki Zen[a*], Koji Suzuki[a], Shigetomo Shiki[a], Masahiro Ukibe[a], Alessandro Casaburi[b], Mikkel Ejrnaes[b], Roberto Cristiano[b], Masataka Ohkubo[a]

[a]*National Institute of Advanced Industrial Science and Technology (AIST), Tsukuba 305-8568, Japan*
[b]*The National Research Council of Italy (CNR), Pozzuoli 80078, Italy*

Abstract

Recently, various types of superconducting detectors have been applied to time-of-flight mass spectrometers (TOF MS) because they can achieve 100 % detection efficiency for a wide mass range from atoms to huge biomolecules. The wide mass range coverage is impossible with conventional microchannel plate (MCP) ion detectors. Superconducting stripline detectors (SSLD) that consist of several hundreds of superconducting nanostrips with a width of < 1 μm and a thickness of a few tens nm have a high sensitivity for biomolecules and a response time of ~ 1 ns that cannot be achieved by other superconducting detectors. For the practical use of SSLD, an easy operation system is necessary. In this study, we will present the proper operation of SSLD which is mounted on a cryogen-free pulse tube cryostat.

Keywords: TOF MS; time-of-flight; SSLD; superconducting stripline detector; cryogen-free; honeycomb collimator

1. Introduction

We have been developing superconducting stripline detectors (SSLDs) for the purpose of measuring the molecular weight of biomolecules such as peptides or proteins in time-of-flight mass spectrometry (TOF MS) [1-3]. Ionized biomolecules are accelerated by high voltage, and by measuring the *tof* of the molecular ions, their mass to charge ratio (*m/z*) are determined. Conventionally, microchannel plate (MCP) detectors have been used to detect molecular ions. Although the MCP detectors have fast timing resolution less than ns, their detection efficiency get degraded with increasing mass. For example, against the bombardment of bovine serum albumin (BSA) whose molecular weight is 66,000 Da (Da corresponds to atomic mass unit.), the possibility of emitting one secondary electron from MCP is only 1 % [4]. On the other hand, SSLD can detect ions at 100 % detection efficiency independent of mass of molecules due to tiny binding energy of cooper pairs of ~ meV compared to tens of keV acceleration energy of TOF MS. This advantage makes the combination of TOF MS and SSLD a powerful tool to cover a wide mass range from light peptides to giant proteins at high sensitivity and high time resolution of less than ns. For the practical use of SSLD with TOF MS, however, an easy operation system is desirable. In other words, an apparatus which can be controlled by researchers who are not familiar with cryogenics is necessary. In this study, we will present the proper operation of

* Corresponding author. Tel.: +81-29-849-1016; fax: +81-29-861-5881 .
E-mail address: n.zen@aist.go.jp .

1875-3892 © 2012 Published by Elsevier B.V. Selection and/or peer-review under responsibility of ISS Program Committee
Open access under CC BY-NC-ND license. doi:10.1016/j.phpro.2012.03.484

SSLD which is mounted on the cryogen-free cryostat, along with the static characteristics of SSLD with a detection area of 1×1 mm^2.

2. Instrument

Figure 1 shows the schematic image of our TOF MS – SSLD apparatus. We have remodeled Voyager DE-STR (Life Technologies corp.). A molecular ion is ionized by matrix assisted laser desorption/ionization (MALDI) which employs N_2-laser for the matrix ablation. (Matrix is a compound of light-weight molecules which can hold the target heavy molecules.) The ionized molecules are accelerated by high voltage of 20 kV. At the acceleration part, the delayed extraction (DE) can be applicable in order to align residual kinetic energies of molecules and obtain better timing resolution. Furthermore, our TOF MS is operated by the reflectron mode and timing resolution can be enhanced again here. An official energy resolution for Insulin (5,807 Da) using MCP is $m/\Delta m$ = 20,000.

SSLD is mounted on the cryofinger of the cryogen-free cryostat. The cryofinger is connected to the 3 K stage of the cryostat through thick and wide bundles made of oxgen-free copper. A honeycomb collimator is attached to the 50 K-radiation shield and settles above the detector [5]. The collimator is made of aluminum with a thickness of 0.015 mm and the pitch of 0.9 mm. The size of through holes of the collimator is large enough for the molecules invasion and effective to block the 300 K-blackbody radiation. Figure 2 shows the comparison of the temperature with and without the honeycomb collimator. The collimator successfully suppressed the temperature of the tip of the cryofinger for more than 250 mK. The temperature of the 3 K stage didn't change significantly. As shown from Fig. 2, the cryostat reaches the base temperature in 16 hours after pushing the button to cool. The base temperature will last forever as long as the cooling water and the electrical power last. (At least, 1 week was confirmed by actual running.)

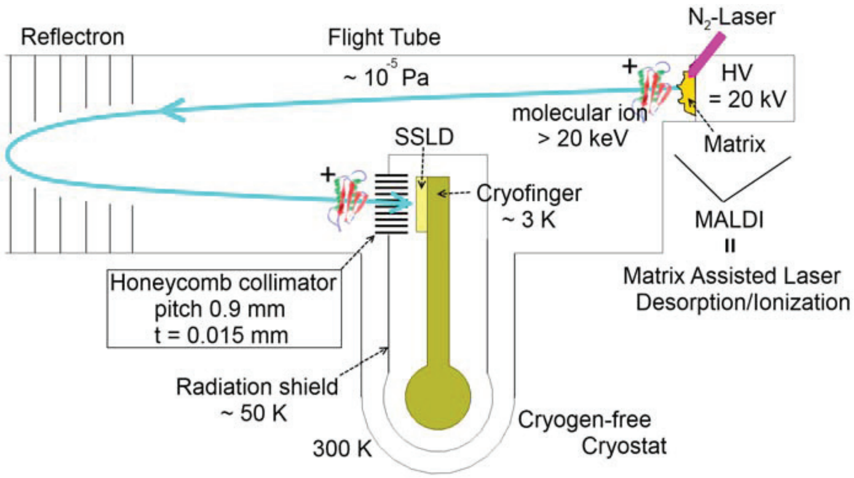

Fig. 1. A schematic image of Matrix Assisted Laser Desorption/Ionization (MALDI) TOF MS, connected with a cryogen-free cryostat. MALDI-TOF MS is operated in the reflectron mode. SSLD is mounted on the tip of the cryofinger of which temperature is around 3 K. A honeycomb collimator is set above the detector at the 50 K-radiation shield and blocks the 300 K blackbody radiation.

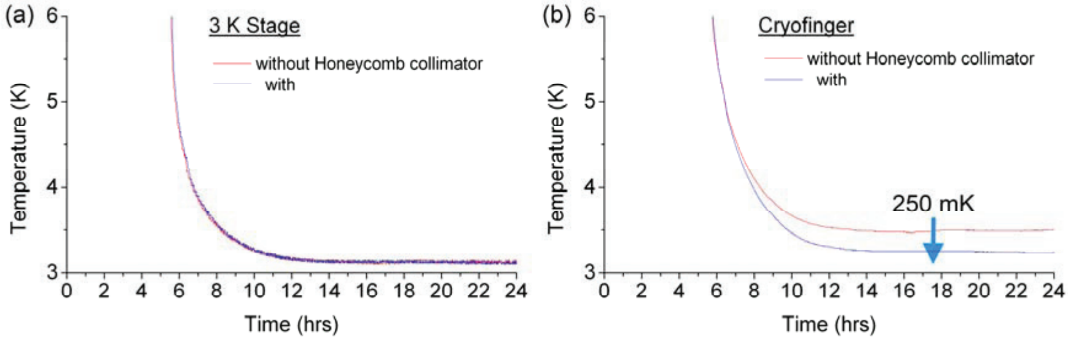

Fig. 2. Measured temperature of (a) 3 K stage and (b) cryofinger with and without the honeycomb collimator.

3. I-V characteristics of 1×1 mm² SSLD

The response time of less than 1 ns with the detection area of 1×1 mm² is achieved by the parallel configuration as shown in Fig. 3 [3]. Because the response time of SSLD is determined by the kinetic inductance of the superconducting stripline [6], the parallel configuration is effective to increase the number of striplines (detection area) without increasing the kinetic inductance [7]. We have tested two parallel SSLDs which have different number of lines in one block, 5 (a) and 10 (b). The 5- and 10-parallel SSLD has 100 and 50 blocks, respectively, and both of them have the same detection area of 1×1 mm². If the number of striplines in one block is expressed by *n*, the kinetic inductance $L_K^{parallel}$ can be expressed by,

$$L_K^{parallel} = \mu_o \lambda_{eff}(T)^2 l/wdn^2, \quad (1)$$

where $\lambda_{eff}(T)$ is the temperature-dependent effective magnetic penetration depth, *l* is the total stripline length, and *w* and *d* are the stripline width and thickness, respectively. Hence, the 10-parallel SSLD has a smaller kinetic inductance than the 5-parallel one. For these SSLD with large detection area, not only the kinetic inductance but also magnetic inductance should be taken into account. However, calculations showed that the 10-parallel SSLD had a smaller magnetic inductance, as well [3]. Consequently, in terms of the response time, the 10-parallel SSLD is superior to the 5-parallel one. Another difference between the 5- and 10-parallel SSLD is the necessary amount of current to drive. As a matter of course, SSLD with the larger number of parallel stiriplines in one block demands more current. The width of the plug (jointing part of striplines) should be determined as the bias current never exceeds the critical current at the plug, and designed to be 25 μm. The width seems wide enough if the width of one stripline of 1 μm is considered.

Figure 4 shows the I-V characteristics of the (a) 5- and (b) 10-parallel SSLD measured by mounted on the cryogen-

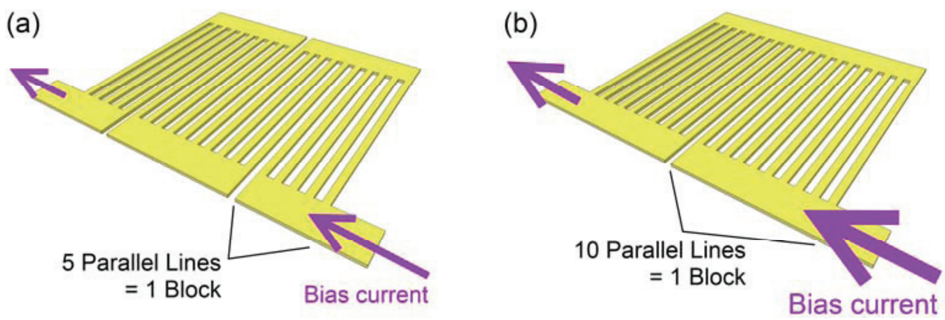

Fig. 3. (a) The 5- and (b) 10-parallel SSLD. The 5- and 10-parallel SSLD has 100 and 50 blocks, respectively. Both of them have the same detection area of 1×1 mm².

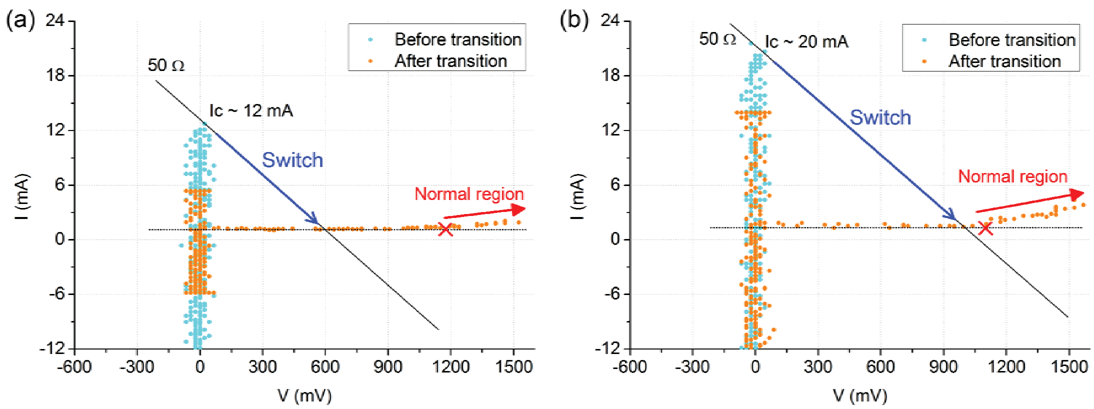

Fig. 4. I-V characteristics of the (a) 5- and (b) 10-parallel SSLD. Cyan and orange color dots are taken just before and after the transition, respectively. If SSLD is biased at I_c in an extreme case, SSLD switches along the 50 Ω-load line (black solid line) by an ion impingement, as indicated by the blue arrow. Horizontal black dot lines are guide to eyes.

free cryostat. Since the parallel-configured SSLD demands typically tens of mA to drive, when it turns to the normal state, a huge amount of joule heating occurs and SSLD never returns to the superconducting state. Therefore, current was applied slowly by slowly to obtain cyan color dots (superconducting state) in Fig. 4, and I_c of 12 mA and 20 mA is obtained for the 5- and 10-parallel SSLD, respectively. Immediately after, I-V curves changed to orange color dots. By interpolating 50 Ω-load line (black solid line in Fig. 4) which corresponds to the impedance of the readout circuit (pre amplifier) in *tof* measurement, we can estimate the stability of the detector during the ion detection measurement. If SSLD is biased at the critical current (in an extreme case) and an ion hits the SSLD, it switches along the 50 Ω-load line as indicated by the blue arrow. By the switching, the 10-parallel SSLD (Fig. 4b) approaches quite close to the normal state which is indicated by the red cross point in the figure. On the other hand, for the 5-parallel SSLD, the 50 Ω-load line intersects with orange dots at the point much far from the normal region. Therefore, the 5-parallel SSLD is superior to the 10-parallel one in terms of the thermally operation stability.

4. Conclusion

We have mounted 1×1 mm^2 parallel-configured SSLDs on the 4 K cryogen-free cryostat which is connected to the high-performance MALDI-TOF MS. Easy cooling operation has been achieved and the honeycomb collimator has turned out to be effective to block the blackbody radiation. In terms of the response time, the 10-parallel SSLD is superior to the 5-parallel one. However, the *I-V* characteristics indicated an unstable operation in the 10-parallel SSLD. It is necessary for optimizing operation condition. In the near future, we will report the performance of SSLD in the high-performance TOF MS with reflectron.

Acknowledgements

We thank the members of the AIST Nano-Processing Facility (AIST-NPF) for device fabrication. This work was supported by a Grant-in-Aid for Scientific Research (A), Japan Society for the Promotion of Science (No. 22246056).

References

[1] Casaburi A, Ejrnaes M, Zen N, Ohkubo M, Pagano S, Cristiano R. *Appl Phys Lett* 2011;98;023702-3.

[2] Suzuki K, Ohkubo M, Ukibe M, Chiba-Kamoshida K, Shiki S, Miki S, Wang Z. *Rapid Commun Mass Spectrom* 2010;24;3290-7.

[3] Zen N, Casaburi A, Shiki S, Suzuki K, Ejrnaes M, Cristiano R, Ohkubo M. *Appl Phys Lett* 2009;95;172508-3.

[4] Westmacott G, Frank M, Labov SE, Benner WH. *Rapid Commun Mass Spectrom* 2000;14;1854-8.

[5] Shiki S, Ukibe M, Shimizugawa Y, Maeda R, Ohkubo M. *J Low Temp Phys* 2008;151;495-5.

[6] Kerman AJ, Dauler EA, Keicher WE, Yang JKW, Berggren KK, Gol'tsman G, Voronov B. *Appl Phys Lett* 2006;88;111116-3.

[7] Ejrnaes M, Cristiano R, Quaranta O, Pagano S, Gaggero A, Mattioli F, et al. *Appl Phys Lett* 2007;91;262509-3.